JOURNAL OF GEOPHYSICAL RESEARCH, VOL. 106, NO. A11, PAGES 25,503–25,516, NOVEMBER 1, 2001

Transients at the dusk side magnetospheric boundary: Surface waves or isolated plasma blobs?

J. De Keyser, F. Darrouzet, and M. Roth

Belgian Institute for Space Aeronomy, Brussels, Belgium

O. L. Vaisberg[1], N. Rybjeva, V. Smirnov, and L. Avanov

Space Research Institute, Moscow, Russia

Z. Nemecek and J. Safrankova

Faculty of Mathematics and Physics, Charles University, Prague, Czech Republic

Abstract. We revisit Interball-Tail and Magion-4 observations of the dusk side magnetospheric boundary on February 15–16, 1996. The observed transient behavior of the boundary can be interpreted in terms of surface waves or as the manifestation of isolated magnetosheath plasma entities embedded in the magnetosphere. We examine the arguments for each of these interpretations with high time resolution magnetic field and plasma data and by exploiting the dual-satellite nature of the observations. We find strong evidence for magnetic field and flow vortices near the magnetospheric boundary and hence for the existence of flux tubes with helicoidal field lines; such structures can be associated with both interpretations. The cross-correlation between the dual satellite observations and the apparent periodicity strongly suggest a Kelvin-Helmholtz surface wave, although other interpretations are not impossible. In any case, the observations for this particular event allow us to derive constraints on surface wave generation mechanisms and on scenarios that could account for the presence of isolated plasma elements in the magnetosphere.

1. Introduction

Mass transfer across the magnetospheric boundary remains a central issue in magnetospheric physics because of its far-reaching implications for the dynamics of the magnetosphere. The interpretation of observations of the magnetopause/low-latitude boundary layer (MP/LLBL), however, is difficult as in situ observations at one or a few points do not allow to unambiguously reconstruct the time-dependent, three-dimensional geometry. This is especially true at the magnetospheric flanks, where transient phenomena are often observed, for instance, multiple magnetic field rotations and/or repeated encounters with magnetosheath-like plasma inward of the magnetospheric boundary. There are two different explanations for such phenomena: (1) The magnetospheric boundary moves back and forth with speeds up to 50 km s^{-1} [*Berchem and Russell*, 1982; *Phan and Paschmann*, 1996], faster than the typical radial spacecraft velocity. This can lead to multiple encounters with the MP/LLBL. Near the subsolar magnetopause, such oscillations are the result of dynamic pressure variations in the magnetosheath [e.g., *Hubert et al.*, 1998]. Farther away from the subsolar point, pressure variations lead to surface waves that are convected tailward with the magnetosheath flow [*Sibeck*, 1990]. Surface waves can also be generated when solar wind conditions are fairly stable, for instance, by the Kelvin-Helmholtz instability when the flow shear across the magnetospheric boundary is large [*Sckopke et al.*, 1981; *Miura and Pritchett*, 1982; *Kivelson and Chen*, 1995; *Fitzenreiter and Ogilvie*, 1995; *Fairfield et al.*, 2000]. The relative importance of solar wind pressure variations and the Kelvin-Helmholtz instability depends on the position on the magnetopause as well as on the interplanetary conditions [*Song et al.*, 1988; *Seon et al.*, 1995]. (2) Repeated encounters with magnetosheath plasma are also possible when magnetosheath material crosses the magnetospheric boundary in the form of plasma blobs or filaments that may or may not remain geometrically connected to the LLBL and/or magnetically connected to the magnetosheath. Possible mechanisms include patchy and transient reconnection (e.g., flux transfer events [*Russell and Elphic*, 1978, 1979; *Berchem and Russell*, 1984] and disconnected magnetosheath transfer events [*Vaisberg et al.*, 1998]) and impulsive penetration [*Lemaire and Roth*, 1978,

[1]Also at Marshall Space Flight Center, Huntsville, Alabama.

Paper number 2001JA900044.
0148-0227/01/2001JA900044$09.00

1991; *Echim and Lemaire*, 2000]; both mechanisms may be related [*Schindler*, 1979]. Isolated plasma structures can also be created near surface waves [*Huba*, 1996b; *Otto and Fairfield*, 2000].

The debate regarding plasma entry mechanisms at the magnetopause is still going on (see *Sibeck et al.* [1999] for an overview), in part because of the absence of complete simulations. For instance, the consequences of merging-type scenarios have been explored but without explanation of why and where merging is initiated [*Ku and Sibeck*, 2000]. Impulsive penetration has been studied up to now only in a two-dimensional subsolar magnetopause setting and without properly accounting for the polarization electric field that drives the penetration [*Ma et al.*, 1991; *Huba*, 1996a; *Savoini et al.*, 1994]. Kelvin-Helmholtz simulations have become more mature but are still limited in the number of spatial dimensions; they usually do not include coupling to the ionosphere, and they employ an ad hoc resistivity [*Huba*, 1996b; *Otto and Fairfield*, 2000].

The lack of multispacecraft observations also has hampered progress in this field. It was hoped that Interball-Tail/Magion-4 dual satellite observations could help to resolve these issues. Such observations have indicated surface motion in several cases [*Safrankova et al.*, 1997]. *Sibeck et al.* [2000] found a number of boundary crossings by the satellite pair to be consistent with surface waves. They found no negative radial density gradients and hence saw no evidence for detached plasma entities. In a case study, *Vaisberg et al.* [1998] reported equatorial dusk side observations of what they interpreted to be isolated structures on closed field lines inside of and close to the magnetospheric boundary, believed to be created by nonsteady, spatially localized reconnection. The conclusions by Sibeck et al. and Vaisberg et al. regarding the occurrence of isolated blobs might appear contradictory. The survey by Sibeck et al. covers 11 passes and relies on measurements of the flux along the Earth-Sun line rather than of the density: Isolated plasma entities are braked in the magnetosphere and eventually come to rest, such that their flux signature vanishes. Such entities are also expected to stretch along the field lines, leading to a reduction in density and again weakening the signature in flux data. The isolated structures reported by Vaisberg et al. on a single pass are much less dense than the magnetosheath, and their imprint on the flux is rather small.

The present paper aims at a further clarification of these issues by revisiting in detail the dusk side MP/LLBL crossing by Magion-4 and Interball-Tail on February 15–16, 1996, reported by *Vaisberg et al.* [1998]. We show that the transients observed during this crossing that were previously interpreted as isolated structures can be understood in terms of a surface wave as well. The prime goal of this paper is to gather evidence that helps to identify the geometry of the magnetospheric boundary. A secondary goal is to derive information regarding the mechanisms that could have produced this geometry. In section 2 we present the observations and data analysis techniques. In section 3 we interpret the observations in the framework of the surface wave and of the isolated plasma entity geometries. We summarize the arguments in favor of each interpretation in section 4.

2. Observations

Interball-Tail and Magion-4 are part of the Russian Interball mission. They were launched in August 1995 into a common highly elliptical orbit (perigee 12,000 km, apogee 200,000 km) with a period of 95 hours and an inclination of 62.8°. We focus here on an inbound dusk side magnetospheric boundary crossing by both satellites on February 15–16, 1996. Wind, well ahead of the Earth's magnetosphere, recorded steady solar wind conditions and an interplanetary magnetic field that did not change much in magnitude nor direction. This picture is confirmed by IMP-8, immediately upstream of the magnetosphere. At the same time, Geotail was also on the dusk side. It moved from the solar wind into the magnetosheath through a bow shock crossing at a shallow angle (threefold crossing near 2208, 2214, and 2234 UT). Geotail observed constant magnetosheath velocities fluctuating only ± 5 km s^{-1} and densities and temperatures varying $\pm 10\%$ or less. Interball-Tail and Magion-4 both recorded stable magnetosheath conditions prior to their passage through the magnetospheric boundary.

Interball-Tail samples the magnetic field at 1 Hz with the 3-axis fluxgate magnetometer MIF [*Klimov et al.*, 1995]. Ion density n^+, temperature T^+, and velocity $\mathbf{V}$ are provided by Interball Tail's SCA-1 instrument [*Vaisberg et al.*, 1995], which obtains three dimensional (3-D) distributions for 0.05–5.0 keV q^{-1} ions with a time resolution of $\sim$10 s, while electron (0.01–26 keV) data are given by the quasi-3-D ELECTRON instrument every spin period (120 s) [*Sauvaud et al.*, 1995, 1997]. The VDP instrument on Interball-Tail and VDP-S on Magion-4 both rely on large-aperture Faraday cups to provide high time resolution (up to 1 s, depending on instrument mode) omnidirectional integral ion fluxes (0.2–0.4 keV) [*Safrankova et al.*, 1997].

Figure 1 highlights the overall structure of the magnetospheric boundary crossing between 2100 UT, February 15, and 0100 UT, February 16, 1996, which took place near 27°N geomagnetic latitude and 1855 geomagnetic local time. Magion-4 was leading Interball-Tail by 2330 s, corresponding to an inward distance of 0.62 R_E. Figure 1a shows the tailward ion flux from SCA-1 on Interball-Tail $f_{\mathrm{IT}}^{\mathrm{SCA}} = -n^+ V_x^{\mathrm{GSE}}$. Figures 1b and 1c plot the tailward ion fluxes $f_{\mathrm{IT}}^{\mathrm{VDP}}$ and $f_{\mathrm{M4}}^{\mathrm{VDPS}}$ from VDP and VDP-S (cross-calibrated scales are used for both). The difference between $f_{\mathrm{IT}}^{\mathrm{SCA}}$ and $f_{\mathrm{IT}}^{\mathrm{VDP}}$ gives an idea of the accuracy. The difference $f_{\mathrm{IT}}^{\mathrm{VDP}} - f_{\mathrm{M4}}^{\mathrm{VDPS}}$ is proportional to the radial gradient (Figure 1d). For later use, we plot the outward plasma velocity V_n normal to the average magnetopause orientation and its time-integrated value $\Delta x_n = \int V_n dt$ in Figures 1e and 1f. Figure 2 gives an overview of the Interball-Tail observations: the magnetic field magnitude and its GSE components (Figures 2a–2d), the GSE ion velocity components (Figures 2e–2g), the ion and electron densities n^+ and n^- (Figure 2h), and the ion and electron temperatures T^+ and

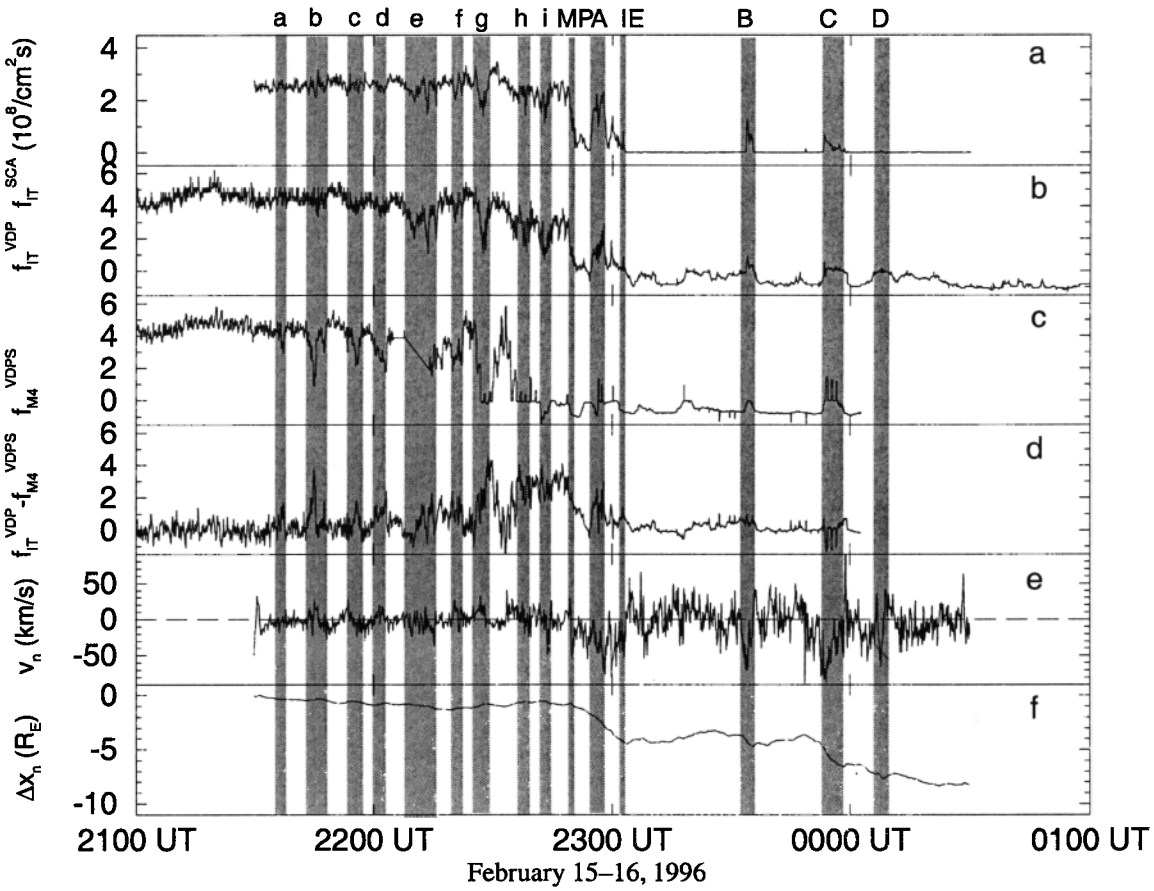

Figure 1. Overview of Magion-4 and Interball observations during the inbound equatorial dusk side magnetopause crossing on February 15–16, 1996: (a) tailward ion flux $f_{\mathrm{IT}}^{\mathrm{SCA}}$ from the SCA-1 spectrometer on Interball-Tail, (b) tailward ion flux $f_{\mathrm{IT}}^{\mathrm{VDP}}$ from VDP on Interball-Tail, (c) tailward ion flux $f_{\mathrm{M4}}^{\mathrm{VDPS}}$ from VDP-S on Magion-4, (d) the difference $f_{\mathrm{IT}}^{\mathrm{VDP}} - f_{\mathrm{M4}}^{\mathrm{VDPS}}$, (e) the velocity V_n in the average boundary normal direction, and (f) its time-integrated value Δx_n (see text). Magion-4 leads Interball-Tail along the orbit by 2330 s. The magnetopause (MP), the LLBL inner edge (IE), and the transient events discussed in the text are indicated.

T^- (Figure 2i). The SCA-1 data suggest $n^+ < 0.2$ cm^{-3} and $T^+ \approx 10^7$ K ≈ 1 keV in the magnetosphere. SCA-1 resolves the cold magnetosheath velocity distributions very well, but it misses the high-energy part of the ion spectra in the magnetosphere. The CORALL instrument aboard Interball-Tail, a 10°×150° aperture spectrometer that scans the sky every spin period to obtain quasi-3-D ion spectra in the energy range 0.030–24.2 keV q^{-1} [*Yermolaev et al.*, 1997], suggests the more realistic magnetospheric values $n^+ \approx 0.35$ cm^{-3} and $T^+ \approx 5$ keV. CORALL, however, misses part of the sky along the spin axis (sunward and anti-sunward directions), which is troublesome in the magnetosheath and in the solar wind. The magnetosheath ELECTRON data are affected by satellite charging and by the difficulty of distinguishing the photo-electrons (up to ~15 eV) from the thermal electrons. The magnetospheric electron spectra, on the contrary, are well resolved and the photo-electrons can easily be subtracted.

Magion-4, being closest to Earth, is the first to record a transient flux decrease (marked a in Figure 1) near the magnetospheric boundary around 2135 UT. Subsequent transients b, c, d, e, and f are observed by both satellites as the flux decreases briefly but are more pronounced at Magion-4. Interball-Tail observes three further flux decreases g, h, and i, near 2228, 2238, and 2243 UT. *Vaisberg et al.* [1998] identify the large magnetic field rotation (~160°) and the corresponding changes in plasma density and temperature at Interball-Tail near 2250 UT as the magnetopause (MP), while the change from magnetosheath to magnetospheric velocity at ~2303 UT, coincident with the transition to magnetospheric density, corresponds to the LLBL inner edge (IE). The beginning of event g seems to be the MP at Magion-4, the first large drop of the tailward flux, but we cannot confirm this in the absence of magnetic field observations (owing to problems with despinning the Magion-4 data). In between the flux decreases g and h observed at Interball-Tail, Magion-4 sees a return to the magnetosheath flux level. Event h coincides with the end of this high flux, and VDP-S records magnetospheric flux levels from the time of event i on, indicating the IE at Magion-4. After having crossed

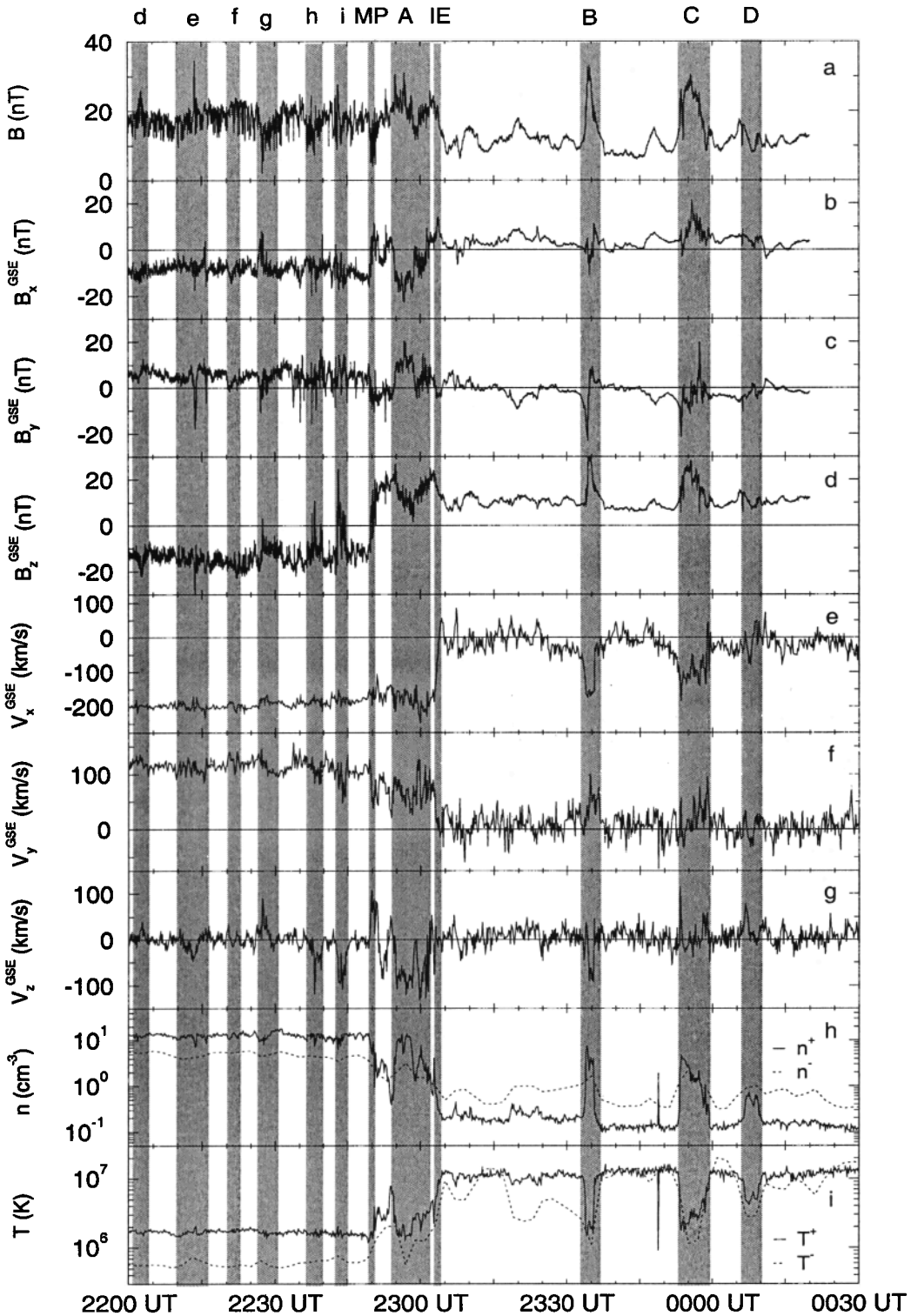

Figure 2. Plasma and magnetic field observations by Interball-Tail during the magnetopause crossing on February 15–16, 1996: (a) magnetic field magitude, (b,c,d) its GSE components, (e,f,g) GSE ion velocity components, (h) ion and electron densities, and (i) ion and electron temperatures. The magnetopause (MP), the LLBL inner edge crossing (IE), and the transient events are indicated.

the magnetopause, Interball-Tail observes four distinct structures around 2300, 2335, 2355, and 0008 UT, which Vaisberg et al. labeled A–D. These structures are visible in the SCA-1, ELECTRON, and VDP data. Note that the VDP fluxes are plotted on a linear scale in Figure 1, while Figure 2h uses a logarithmic scale for the plasma densities. There are corresponding features at Magion-4 for events A, B, and C (VDP-S data are missing for event D). Figures 3a and 3b plot the magnetic field and the SCA-1 ion velocity, projected onto the GSE x-y plane, along the common space-

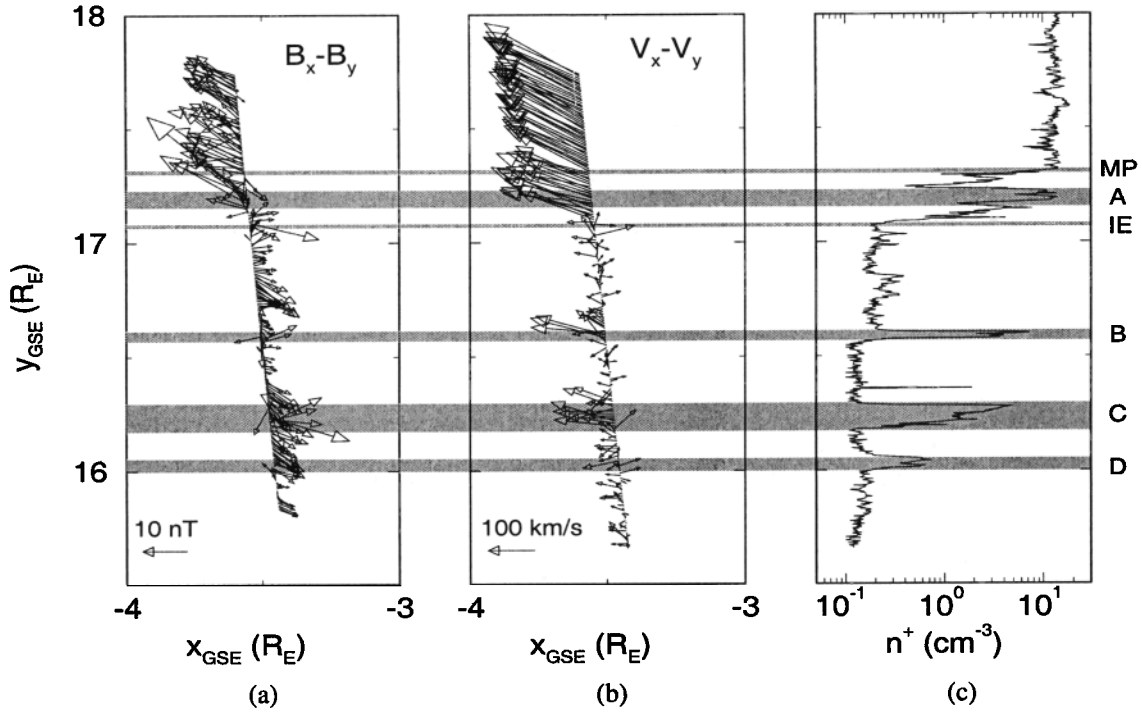

Figure 3. Interball-Tail data during February 15–16, 1996, MP/LLBL crossing: (a) magnetic field vectors projected onto the GSE x-y plane, plotted along the inbound spacecraft orbit, (b) ion velocity projected onto the GSE x-y plane, plotted along the orbit, and (c) ion density profile. Transients A, B, C, and D, the magnetopause (MP) and the LLBL inner edge (IE) are indicated.

craft trajectory with ~40 s resolution. Figure 3c plots the ion density as a function of y_{GSE}. (The GSE z velocity is negligible as the crossing occurs near the equator.) The tailward motion of the magnetosheath-like plasma observed during transients B and C amidst the essentially stationary magnetospheric plasma can easily be distinguished.

We assume that the observed transients are essentially time-stationary structures that are convected past the satellites. For every plasma discontinuity, at the beginning and end of transients g, h, i, A, B, C, and D, at the MP, and at the IE, we have computed the minimum variance frame (MVF) and the corresponding surface normals from the Interball-Tail MIF data; α, β, and γ denote the mimimum, intermediate, and maximum variance directions, respectively. As the discontinuity traversals can be brief and as they are not always accompanied by a strong magnetic field signature, the statistical significance of the principal axes returned by the MVF analysis sometimes is poor, a problem called "degeneracy" [*Sonnerup and Scheible*, 1998]. In such cases, we add the a priori constraint that the interface is a tangential discontinuity (TD). We then rotate the MVF around the maximum variance axis (which turns out to be always well-defined) such that the normal magnetic field is zero (a variant of techniques described by *Sonnerup and Scheible* [1998]). The resulting reference frame is referred to as the tangential discontinuity frame (TDF). For each discontinuity, Table 1 lists the GSE normal $\mathbf{n}$ and the variances $\lambda_{\alpha,\beta,\gamma}$ associated with each principal axis of the magnetic field covariance matrix. The TD assumption is justified a posteriori by the systematically small normal field B_α (zero within the one-sigma level) when MVF analysis provides statistically significant principal axes. The maximum variance direction is always well-defined ($\lambda_{\alpha,\beta} < \lambda_\gamma$), and it always points more or less along GSE z ($n_z < n_{x,y}$): The observed structures are essentially parallel to the magnetospheric field. The same conclusion is reached by conducting a minimum variance analysis of the vector $\mathbf{n} = \mathbf{B} \times \delta\mathbf{B}$ for the entire crossing ($\delta\mathbf{B}(t_k) = \mathbf{B}(t_{k+1}) - \mathbf{B}(t_{k-1})$ is the central difference of the magnetic field time series); this is a variant of the basic MVF techniques [*Sonnerup and Scheible*, 1998; *Song and Russell*, 1999]. If the curved structures are field aligned, $\mathbf{n}$ is the local surface normal, both perpendicular to the magnetic field and to changes in the field vector. This normal vector analysis confirms that $\mathbf{n}$ remains confined to the GSE x-y plane throughout the boundary crossing; for this reason we present Figures 2 and 3 in GSE coordinates. The angle ϕ in the last column of Table 1 gives the azimuth of the surface normals in the GSE x-y plane. The average MP normal azimuth is ~53°; the flaring angle is ~37°. The interfaces around structures g, h, i, and A bracket or are close to this azimuth, while those around B, C, and D deviate strongly from the mean MP orientation.

Figure 4 zooms in on the Interball-Tail MP crossing. Figure 4 (left) shows the MVF magnetic field components. The large field rotation is interrupted several times by brief dips in the B_γ component, during which B_α and B_β show characteristic variations indicative of nonplanar small-scale structure. These features can be interpreted as small-scale undulations of the magnetopause. They show up in the B_β,B_γ hodogram (Figure 4, right) as repeated closed loops.

Table 1. Interface Normals for the Interball-Tail Crossing on 15–16 February, 1996 [a]

Event	UT	Method	B_α/B	$\lambda_{\alpha,\beta}/\lambda_\gamma$	$n_{x,y,z}$	ϕ, deg
g	2227	MVF	0.03±0.06	0.02, 0.16	(0.37, 0.93, 0.04)	68
g	2228	MVF	0.02±0.10	0.06, 0.12	(0.61, 0.79, −0.04)	52
h	2238	TDF	±0.06	0.02, 0.02	(0.62, 0.78, −0.12)	52
h	2238	TDF	±0.13	0.08, 0.10	(0.59, 0.76, −0.29)	52
i	2243	TDF	±0.12	0.02, 0.02	(0.45, 0.89, 0.04)	63
i	2243	TDF	±0.11	0.03, 0.05	(0.60, 0.79, −0.15)	52
MP	2250	MVF	0.13±0.12	0.03, 0.10	(0.60, 0.79, −0.12)	53
A	2254	MVF	0.13±0.09	0.04, 0.12	(0.63, 0.77, −0.06)	51
A	2258	TDF	±0.12	0.08, 0.08	(0.62, 0.78, −0.03)	52
IE	2303	TDF	±0.11	0.06, 0.09	(0.52, 0.83, −0.20)	58
B	2334	MVF	0.01±0.16	0.02, 0.30	(0.96, 0.23, 0.14)	13
B	2335	MVF	0.30±0.12	0.03, 0.14	(0.31, 0.94, −0.13)	72
C	2253	MVF	0.24±0.14	0.05, 0.50	(0.97, 0.23, 0.10)	13
C	2258	TDF	±0.30	0.39, 0.13	(0.25, 0.92, 0.29)	105
D	0006	TDF	±0.07	0.10, 0.15	(0.88, 0.38, 0.27)	23
D	0009	MVF	0.14±0.06	0.03, 0.08	(0.63, 0.78, 0.02)	51

[a] For each interface (indicated in Figure 2) the table lists the time (UT), the variance analysis method (MVF or TDF, see text), the relative normal magnetic field B_α/B, the variance ratios $\lambda_\alpha/\lambda_\gamma$ and $\lambda_\beta/\lambda_\gamma$ ($\lambda_\alpha \leq \lambda_\beta \leq \lambda_\gamma$), the interface normal $n_{x,y,z}$ (unit vector in the GSE frame), and its azimuth ϕ (angle with x in the GSE x-y plane).

The MVF normal velocity strongly fluctuates during the traversal; the time resolution is insufficient to track the instantaneous plasma motion. Moreover, the mean normal velocity is strongly dependent on the precise MVF orientation. It is therefore difficult to estimate the true MP thickness. The undulations typically last ~5 s; when taken to correspond to half the wavelength and noting that the flow speed is ~200 km s^{-1} on either side of the MP, one finds a wavelength of ~0.25 R_E. The undulation amplitude is less than the MP thickness as the observed field fluctuations cover only part of the full magnetic field rotation across the MP.

A single-valued ion density/temperature relation is observed throughout the crossing [*Vaisberg et al.*, 1998, Figure 3]. We verified that the electron density/temperature relation is single valued as well. These relations therefore provide no evidence whatsoever for a different thermodynamic history of the particles in the transients.

In order to study the transients more closely, we project the magnetic field and flow vectors observed by Interball-Tail onto the x-y plane of a reference frame that is oriented like the GSE frame but moves with a velocity intermediate between the magnetosheath and the magnetospheric velocities (Figures 5a–5d): $\mathbf{V}^{\text{frame}} = (-110, 45, 0)$ km s^{-1}. In the surface wave scenario, $\mathbf{V}^{\text{frame}}$ approximates the phase velocity of the wave; the waveform should be more or less stationary in this frame. In the case of isolated plasma entities, $\mathbf{V}^{\text{frame}}$ is essentially the speed of the plasma entity for transients B and C (the speed is higher for transient A and lower for D). Note that the geocentric Interball-Tail velocity is comparatively small (1.7 km s^{-1}).

Figure 5a plots the magnetic field (top part, 16 s resolu-

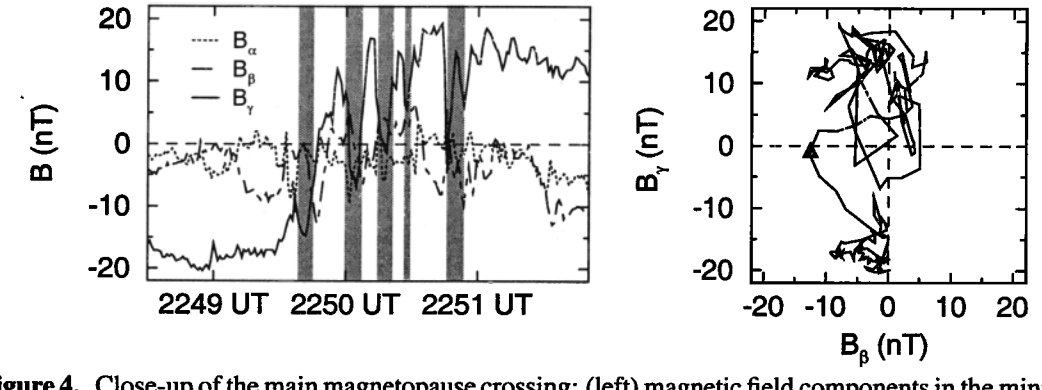

Figure 4. Close-up of the main magnetopause crossing: (left) magnetic field components in the minimum variance frame and (right) magnetic field hodogram. Instead of a monotonically increasing B_γ, there are transient returns to lower B_γ values as indicated by the shading; these transients correspond to closed loops in the B_β, B_γ hodogram.

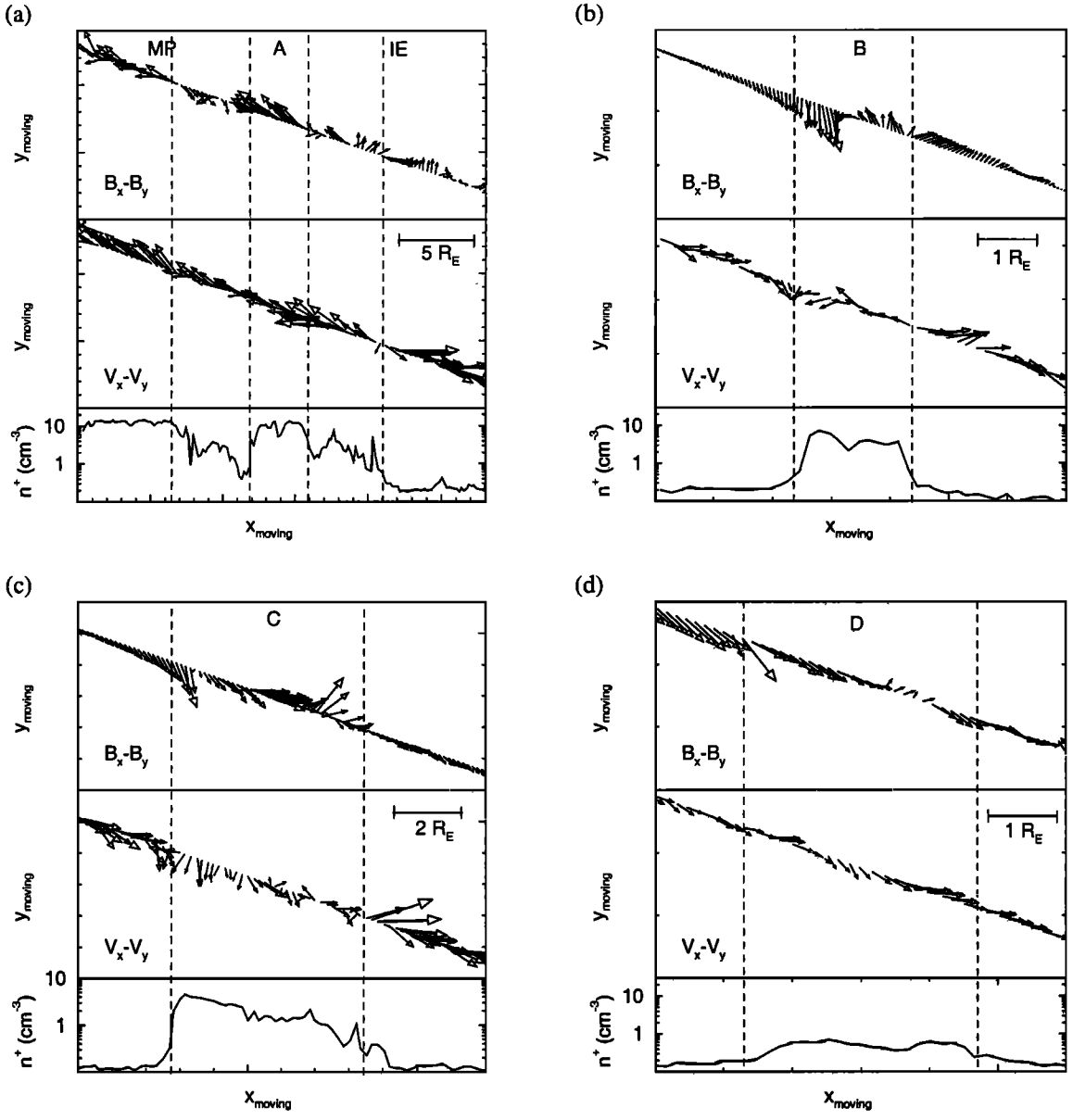

Figure 5. The transients as seen in a reference frame x_{moving},y_{moving},z_{moving} that is oriented like the GSE frame but that moves with a velocity intermediate between the magnetosheath and the magnetospheric plasma flow (see text): x-y projections of the magnetic field vectors (top plots) and ion velocity vectors (middle plots) along the spacecraft trajectory, and the corresponding ion density profiles (bottom plots). (a) Magnetopause crossing (MP), transient A, and inner edge (IE); (b) transient B; (c) transient C; (d) transient D. The scale on which the magnetic field and velocity vectors are drawn is arbitrary.

tion) and velocity vectors (middle part, 20 s resolution), and the ion density (bottom part) during the encounter with the MP, transient A, and the IE, as Interball-Tail passes through the structure from upper left to lower right in the moving reference frame. Before crossing the MP the magnetospheric boundary moves toward the satellite (plasma velocity is outward relative to the trajectory). After crossing the MP and during transient A, the velocity remains tangential to the trajectory: Interball-Tail moves nearly parallel to the boundary. This is also suggested by the constant magnetosheath-like density and reduced B_z inside A (see Figure 2). The surface normals for the MP and for the leading and trailing edges of event A are very similar as well. After event A and up to the IE the flow is again directed outward relative to the trajectory, indicating further relative motion of the satellite toward the magnetosphere. The IE is the point where the flow direction in the moving reference frame changes from tailward to sunward, coincident with the point where the density drops down to the magnetospheric value. Note that the x-y magnetic field is smaller inside the magnetosphere and the LLBL, as the field is mostly along z there. Figure 5b shows the magnetic field and the ion data for transient B (for convenience plotted at 4 s and at 10 s resolution, respectively). Its leading and trailing edges are located where the

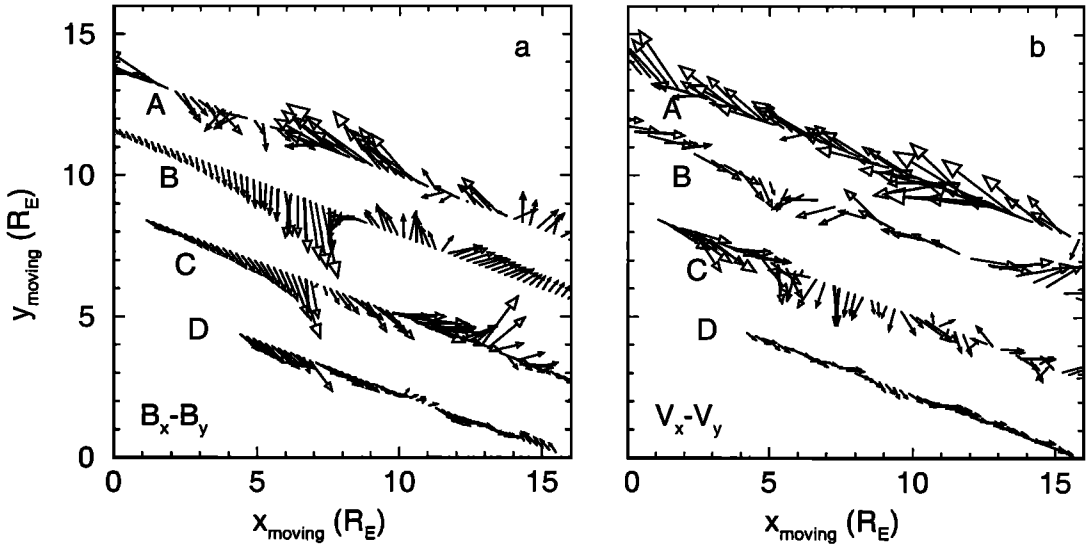

Figure 6. Flux rope topology suggested by juxtaposing data obtained from the four consecutive transients A, B, C, and D: x-y projections of (a) magnetic field and (b) velocity vectors in the moving reference frame x_{moving},y_{moving},z_{moving}. The offsets between the trajectories for each transient were chosen arbitrarily. The vectors for different transients do not have a common scale; this is meant to illustrate only their orientation. The vertical separation between the passes is chosen arbitrarily.

density abruptly changes, at the point where the flow sense in the moving frame changes from sunward to tailward at the leading edge, and back to sunward at the trailing edge. The structure appears to be $\sim 2\,R_E$ wide along the satellite trajectory. The magnetic field shows progressive changes from a considerable distance before to well beyond the structure. The flow inside the transient follows a pattern similar to the magnetic field. The magnetic field points inward at the beginning of transient C (Figure 5c, 8 s magnetic field, 10 s ion data), sunward at its center, and outward at the end of the transient. The flow again mimics the field. Transient D is relatively broad, with only a minor density enhancement (Figure 5d, 8 s magnetic field, 10 s ion data). The flow is always sunward in the moving frame, as expected for primarily magnetospheric plasma. Small fluctuations in the velocity vectors point alternatingly earthward and outward; the behavior of the magnetic field lines is similar.

It is very tempting to interpret the transients as flux ropes aligned with the GSE z axis. The interior of an infinitely long flux rope carrying a uniform current $\mathbf{j}$ along z has a constant magnetic field vorticity (or helicity) $\Psi = \nabla \times \mathbf{B} = \mu_0 \mathbf{j}$ with $\Psi_x = \Psi_y = 0$ and $\Psi_z \neq 0$. The nonzero magnetic field vorticity implies helicoidal field lines that project as closed contours (vortex structure) onto the x-y plane. Although the satellite samples each transient only along a line, the combined picture strongly suggests the existence of closed field line projections in the x-y plane. Figure 6 is a compilation of the observations after scaling; the same scaling was used to construct the $\mathbf{B}$ and $\mathbf{V}$ plots (vectors for different transients have different scales, it is their orientation that matters here). Both $\mathbf{B}$ and $\mathbf{V}$ show similar vortex patterns, consistent with the same rotation sense. During event A the spacecraft passes far from the vortex center, on the magnetosheath side, resulting in antisunward flow. In event B it passes much closer to the vortex center, again on the magnetosheath side, so that the flow remains antisunward. During event C, Interball-Tail passes on the earthward side of the vortex center such that the flow is sunward. Event D represents a pass far from the vortex center on the earthward side. This sequence is precisely what is expected for a satellite that is progressively moving inward. As the four slices correspond to different transients, this reconstruction illustrates what could be a common underlying topology. Since B_z is much stronger than $B_{x,y}$ the pitch angle of the helicoidal lines in the north–south aligned flux rope is large. The flux rope diameter is a few R_E.

3. Geometry: Surface Waves or Isolated Plasma Entities?

In this section we try to construct consistent interpretations in terms of both the surface wave and the isolated plasma entity geometries. In a further step, we discuss the implications on possible formation mechanisms.

3.1. Surface Waves

3.1.1. Geometry. A fundamental observation is the alignment of the transient structures with the GSE z axis, while they display strong curvature in the x-y plane. This would be natural for a surface wave: As the wave vector points tailward with the flow (except perhaps for strong tilted shock fronts or plasma discontinuities that hit the magnetosphere first at some point far from the nose of the magnetopause), the wave crests are north-south aligned [see also *Ivchenko et al.*, 2000]. The fact that the interfaces are parallel to z and that the azimuths of the leading and trailing

edges of transients g, h, i, and A bracket the MP orientation similarly suggests that we repeatedly observe the same undulating structure.

The observed sequence of events can be interpreted as follows (see Figures 1 and 2). Magion-4, being closer to Earth, is the first to reach the MP/LLBL; event a represents a brief passage through a surface wave crest. Subsequent passages (b, c, d, e, f) are deeper as witnessed by the flux decreases of up to 50% recorded by Magion-4, with corresponding smaller flux signatures at Interball-Tail. Magion-4 then crosses the magnetopause, remains some time in the LLBL close to the inner edge as indicated by the near disappearance of the flux, and then moves back outward into the magnetosheath. In the meantime, Interball-Tail sees only a small and brief flux decrease (event g). Magion-4 crosses the MP again to enter the LLBL, coincident with yet another flux decrease at Interball-Tail (event h). Event i, a last flux decrease at Interball-Tail, signals the entry of Magion-4 into the magnetosphere proper, although it is difficult to locate the IE precisely in the VDP-S data. Interball-Tail encounters the MP at a time Magion-4 is still close to the inner edge. While Interball-Tail leaves the LLBL and sees transients A, B, C, and D as transient flux increases when passing through surface wave troughs (motion toward the MP for A, partial reentries into the LLBL for B, C, and D), Magion-4 observes simultaneous but smaller flux enhancements as it is located more earthward. The depth of return into the LLBL progressively decreases from transient B to D, which readily accounts for the trend in density, flow speed, and temperature in the transients as seen by Interball-Tail. In summary, this sequence of events is exactly what one expects for satellites that slowly move earthward and whose separation is about half of the boundary width.

The magnetopause, defined by $B_z \approx 0$, is first observed by Interball-Tail in event g at $Y_{\mathrm{GSE}} = 17.65\,R_E$ and last in event A at $Y_{\mathrm{GSE}} = 17.15\,R_E$, implying an amplitude (trough-to-crest distance) of the MP undulations of $\sim 0.4\,R_E$ when accounting for the 37° average flaring angle and the orientation of the satellite trajectory. The inner edge undulations seen by Interball-Tail between IE at $Y_{\mathrm{GSE}} = 17.1\,R_E$ and the end of transient D at $Y_{\mathrm{GSE}} = 16.0\,R_E$ cover a transverse distance of $0.9\,R_E$. The larger amplitude of the IE undulations is consistent with earlier analyses [*Sckopke et al.*, 1981] and with the small deviations of the surface normals from the average magnetospheric orientation for events g, h, and i, while large deviations were found for B, C, and D (Table 1). An upper limit for the MP/LLBL thickness is obtained as the boundary normal distance between events g and D, being $\sim 1.0\,R_E$. These estimates of wave amplitude and boundary thickness are only valid if the magnetosphere does not significantly expand or contract on average during the crossing interval. A dual-satellite estimate of the instantaneous normal MP/LLBL speed to aid in deriving the boundary thickness, as done earlier with ISEE-1/2 [*Berchem and Russell*, 1982], is not possible here because both satellites are too far apart. Noting that Interball-Tail briefly enters the MP current layer in event a, while Magion-4 then penetrates deeply in the LLBL, we deduce an MP/LLBL

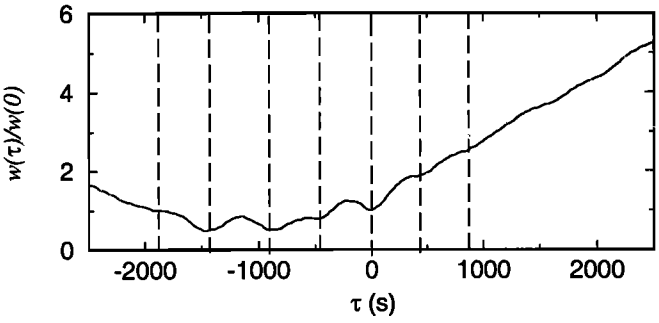

Figure 7. Cross-correlation $w(\tau)$ relative to $w(0)$, the cross correlation at zero time lag, of Interball-Tail/VDP and Magion-4/VDP-S flux measurements (see text for more details), showing several local minima at regularly spaced time delays τ, which are indicative of a common underlying time periodicity.

thickness somewhat larger than the spacecraft separation ($0.6\,R_E$). Interball-Tail observes the MP and transients A, B, and C, when the satellite is inside the LLBL, while Magion-4 remains close to the inner edge, also indicating that the MP/LLBL thickness must be larger than the separation distance in the boundary normal direction. In conclusion, we find the MP/LLBL (which does not have the same thickness everywhere) to be $0.7 - 1.0\,R_E$ thick.

The fact that the separation between the two satellites is less than the boundary thickness is responsible for the apparent correlation between the VDP and VDP-S fluxes. We have performed a cross-correlation analysis between these data. Figure 7 plots $w(\tau) = \int_{t_0-\Delta t}^{t_0+\Delta t} [f_{\mathrm{IT}}^{VDP}(t - \tau/2) - f_{\mathrm{M4}}^{VDPS}(t + \tau/2)]^2 dt$ relative to $w(0)$, where t_0 and Δt are the midpoint and the quarter width of the time window for which we have data from both satellites, and where τ is the correlation delay; the figure shows minima, regularly spaced at ~450 s intervals, that are evidence for surface wave periodicity. It should be noted that $w(\tau)$ mainly reflects the transients before and around the MP crossing, where the flux changes are most pronounced; transients B, C, and D contribute only a little to the cross correlation. The minimum at $\tau = 0$ s corresponds to the correlation of the data recorded simultaneously by both satellites. Both satellites cross the magnetospheric boundary when the surface wave is at a different phase; one therefore does not expect the signatures at both satellites to be identical. For that reason, the cross-correlation analysis is not expected to give a minimum $w(\tau)$ close to zero, even if the periodicity would be perfect. Figure 7 shows that $w(\tau)$ obtains its global minimum for $\tau < 0$: The Interball-Tail data have to be shifted back in time and/or the Magion-4 data have to shift forward in time to achieve the best matching with a shift of 2–3 wave periods. As Interball-Tail lags Magion-4 by 2330 s along the orbit, the phase shift between both should be ~5 periods. This discrepancy can be explained by an overall inward boundary motion during the crossing (evidence for such motion is discussed below; an inward motion of $0.3\,R_E$ can account for a 2–3 period shift in the correlation minimum). The regularly spaced minima indicate that the periodicity is a common un-

derlying characteristic in the measurements from both satellites. Similar values for the wave period show up in the Fourier analysis of f_{IT}^{VDP} and f_{M4}^{VDPS}. During one period both satellites travel over an inward distance that is less than the wave amplitude so that they necessarily must observe at least one full surface undulation between the MP and the IE crossings. Indeed, both observe a sequence MP–transient–IE, whose duration can be used to estimate the wave period directly. With a phase velocity of $\sim$150 km s^{-1}, a period of 450 s (frequency 2.2 mHz) implies a wavelength of $\sim 10\,R_E$ (an upper bound for the lengths of A, B, C, and D, see Figure 5). Note that we earlier found smaller scale undulations ($0.25\,R_E$ wavelength) superposed on this wavy magnetopause.

The vortex structure found earlier (Figure 6) also fits the surface wave geometry: Simulations show vortex patterns in both flow and field (e.g., for Kelvin-Helmholtz waves, see *Otto and Fairfield* [2000, Figure 7]) that are very similar to what we observe here. The earthward motion of the satellites produces successive transits through the vortices at progressively more earthward positions. Simulations [*Miura*, 1995; *Huba*, 1996b; *Otto and Fairfield*, 2000] indicate the possibility of complicated density structures, which might account for the apparent asymmetry between the leading and the trailing edges of transients A, B, and C, with the trailing edges being generally less dense in the Interball-Tail SCA-1 data, a feature discussed by *Vaisberg et al.* [1998]. The ion and electron temperature variations follow the density changes and can be explained by a single-valued density/temperature relation in terms of the changing position of the spacecraft relative to the magnetospheric boundary.

The boundary normal velocity V_n measured by Interball-Tail should have an alternating sign if the surface wave geometry is correct; such fluctuations are present in Figure 1e. They are largest after the main magnetopause crossing. This is consistent with the larger wave amplitudes on the inner edge than on the magnetopause and with the larger Alfvén and sound speeds there. Owing to the lower magnetospheric density, the observational error on the velocity is larger as well. If the plasma would collectively move with a globally expanding/contracting magnetospheric boundary, $V_n(t)$ would reflect this motion and integration over time should then give the changing MP/LLBL position $\Delta x_n(t)$ (Figure 1f). If the boundary motion is a local rather than global movement, however, V_n includes a fraction of the (large) tailward velocity in the magnetosheath because of the changes in local boundary normal orientation, and this leads to an exaggeration of the true boundary normal motion. Additionally, V_n may vary on timescales shorter than those resolved by SCA-1 (10 s) so that its integrated value could be meaningless. That such higher frequency flow variations exist is suggested by the rapid magnetic field variations (such as those observed during the main MP crossing, see Figure 4). Also, a small systematic error in V_n of only 1 km s^{-1} (for instance, owing to not correctly choosing the average boundary normal direction) results after a 3 hour integration in a 1.7 R_E position error. Therefore V_n is at most a qualitative indicator of boundary motion; the plot in Figure 1f does not imply that the boundary has really moved $8\,R_E$ inward during this time period. (In fact, the satellites move inward over only $2.4\,R_E$ during the crossing.) The plot, however, does make clear that there are prolonged periods during which the boundary oscillates around a fixed position, allowing the satellites to cross parts of the MP/LLBL repeatedly. The strong inward displacement between the Interball-Tail MP and IE encounters is not matched by the VDP or VDP-S data; it might be the exaggerated signature of a smaller but real inward shift of the average boundary location. This would explain our earlier finding that the optimal cross-correlation delay is less than the time separation between the two spacecraft.

The observed V_z variations (Figure 2) are interpreted in the surface wave geometry as being parallel to the interfaces. Such a flow should be easy in the LLBL and in the magnetosphere as it is essentially field-aligned there. In some cases this flow might be related to the currents associated with the magnetic field changes.

3.1.2. Formation mechanisms. Surface waves might be generated by a train of solar wind dynamic pressure pulses [*Sibeck*, 1990], but a Kelvin-Helmholtz unstable inner edge is possible as well, as in the traveling LLBL vortices model [*Sckopke et al.*, 1981]. The wavelengths and frequencies observed here are typical for the Kelvin-Helmholtz instability [*Walker*, 1981; *Kivelson and Chen*, 1995] but could also correspond to solar wind pressure variations. Incompressible magnetohydrodynamics predicts that the inner edge becomes Kelvin-Helmholtz unstable [*Ogilvie and Fitzenreiter*, 1989] when

$$[\boldsymbol{k}\cdot(\boldsymbol{V}_{\mathrm{LLBL}}-\boldsymbol{V}_{\mathrm{MSPH}})]^2 > \frac{\rho_{\mathrm{LLBL}}+\rho_{\mathrm{MSPH}}}{\mu_0\rho_{\mathrm{LLBL}}\rho_{\mathrm{MSPH}}}[(\boldsymbol{k}\cdot\boldsymbol{B}_{\mathrm{LLBL}})^2+(\boldsymbol{k}\cdot\boldsymbol{B}_{\mathrm{MSPH}})^2].$$

As the wave vector $\mathbf{k}$ and the shear flow are perpendicular to the magnetic field at the dawn and dusk flanks, the inner edge is very susceptible to the Kelvin-Helmholtz instability there [*Farrugia et al.*, 2000; *Fairfield et al.*, 2000]. For the Interball-Tail plasma parameters and for $\mathbf{k} \parallel \mathbf{V}_{\mathrm{LLBL}}$, this condition becomes $V_{\mathrm{LLBL}} > v_{\mathrm{KH}} = \cos\theta \times 1100$ km s^{-1}, with θ the angle between the magnetic field and the flow in the LLBL. For $\theta = 90°$ the threshold velocity is $V_{\mathrm{KH}} = 0$, while $V_{\mathrm{KH}} = 195$ km s^{-1} when $\theta = 80°$ (stability is enhanced when the flow is not exactly perpendicular to the field). As the observed shear flow is >220 km s^{-1}, the Kelvin-Helmholtz instability is very likely. The pronounced cross-correlation minima at regularly spaced time delays in Figure 7 demonstrate that there is a boundary wave with a well-defined periodicity, again pointing to the Kelvin-Helmholtz instability as most likely mechanism. In any case, the surface wave cannot have been generated much more than 1 wavelength ($10\,R_E$) upstream. It thus cannot have reached the strongly nonlinear regime, so that a simple vortex and density structure is expected (more complicated vortices are observed further downstream [*Otto and Fairfield*, 2000]). The lack of perfect periodicity could indicate the presence of multiple Kelvin-Helmholtz modes and/or solar wind pressure modulation. We inferred the presence of some

solar wind pressure modulation from Figure 1f (although exaggerated there). Solar wind and magnetosheath observations by Wind, IMP-8, and Geotail exclude major total pressure variations.

3.2. Isolated Plasma Entities

3.2.1. Geometry. If the transients are isolated plasma structures, the north-south alignment of all interfaces indicates that these entities are elongated along the field direction rather than quasi-spherical. The events observed prior to the MP crossing can be interpreted as filaments in the process of crossing the magnetopause. For instance, Interball-Tail observes filaments g, h, and i in the magnetosheath, close to the magnetopause, while Magion-4 observes them in the LLBL or in the magnetosphere. Interball-Tail encounters event A in the LLBL, while Magion-4 observes it in the magnetosphere. Events B, C, and D can be regarded as plasma entities observed by both satellites inside the magnetosphere. The directions of the surface normals listed in Table 1 are also fully compatible with this interpretation.

The filaments are a few R_E long in the flow direction (Figure 5). Their transverse extent cannot be more than $\sim 1\ R_E$ since we observe the transients no more than $\sim 1\ R_E$ inward of the MP. The similarities in Interball-Tail and Magion-4 observations imply that the transverse extent is at least $0.6\ R_E$, the satellite separation in the boundary normal direction. The filament cross section would therefore be elongated. The estimated distance between filament center and the magnetopause is not much larger than the transverse extent of the filaments, so that it remains difficult to establish whether the filaments are geometrically isolated from the MP/LLBL.

The filamentary nature of the plasma entities is in agreement with the magnetic field and velocity vortex of Figure 6. Not much is known about the flow pattern to be expected inside plasma filaments that travel through the magnetosphere; the observations presented here always show a vortex with the same sense of rotation. The analogy with hydrodynamics suggests that a plasma wake is formed behind the filaments, which could explain the elongated shape of the transients as well as the asymmetric SCA-1 plasma parameters inside the transients [*Vaisberg et al.*, 1998]; such a wake shows up in simulations [*Ma et al.*, 1991; *Huba*, 1996a].

Table 2 summarizes the average GSE x-y velocities observed by Interball-Tail in the magnetosheath and in the filaments. A peculiar property of the transients is the progressive decrease in flow speed from event A to D, which appears to reflect the braking of the filament. Table 2 also shows how the angle with the x axis becomes smaller for the more earthward filaments, although the uncertainties on the velocities are large. Moreover, it is generally not correct to use the mean velocity observed in a filament as the filament velocity, except when one measures the velocity near the filament center as in transients B and C. Given the magnetosheath and the filament velocity vectors and given the filament distance earthward of the magnetopause, a simple but rough trigonometric estimate of the point where the filament must have crossed the magnetopause can be made by replacing the magnetopause and the filament trajectory projections onto the x-y plane by straight lines. For filament A we find a distance $0.8\ R_E$ upstream, while filament B must have traveled $\sim 3\ R_E$ through the magnetosphere. The observed speeds imply that filament B would have entered the magnetosphere ~ 120 s before being observed.

Table 2. Flow Direction in the Magnetosheath and in Transients A, B, C, and D

Event	V_x^{GSE}, km s^{-1}	V_y^{GSE}, km s^{-1}	Flaring Angle, deg
MSH	-185	109	31
A	-168	67	22
B	-163	48	16
C	-116	-2	−1
D	-21	-9	ill-defined

While events g, h, i, and A show a progressive deviation from the magnetosheath to the magnetospheric magnetic field orientation, the field lines in filaments B, C, and D are helicoidally wound around the magnetospheric field direction. This implies that the magnetospheric field rapidly diffuses into the filaments, in a matter of several tens of seconds. No distinct D-shaped cold ion distributions were found inside these filaments, indicating that they are no longer magnetically connected to the magnetosheath [*Vaisberg et al.*, 1998].

3.2.2. Formation mechanisms. An interpretation in terms of transient reconnection has been given earlier by *Vaisberg et al.* [1998]. The main arguments supporting transient reconnection include the flux-rope structure and the geomagnetic alignment of the FTE flux tube inside the magnetosphere, the progressive density and temperature change, sporadic plasma jetting (seen as brief V_y^{GSE} and V_z^{GSE} excursions), and the antiparallel magnetic field orientation believed to favor reconnection. Transients g, h, and i were ascribed to leakage of magnetospheric particles into the magnetosheath. Transients A, B, C, and D seem to differ from typical FTEs as the absence of D-shaped magnetosheath-like ion distributions indicates that reconnection has ceased. The standard FTE picture does not explain why the innermost FTE flux tubes are not dragged tailward. The transients observed in the magnetosheath before the magnetopause crossing were not discussed by *Vaisberg et al.* [1998]; they can be interpreted as the magnetosheath half of FTE flux tubes. We stress that if transients A, B, C, and D are indeed some type of FTE, then Figure 6 provides clear evidence that tail flank FTEs have a noncircular shape and a rotating core [*Sibeck and Smith*, 1992]. The systematic changes in field direction observed before and after these transients reflect field line draping around FTEs [*Russell and Elphic*, 1979, Figure 2].

Isolated plasma filaments associated with density decreases on the magnetosheath side of the boundary and with density enhancements at the magnetospheric side can also be produced by a nonlinearly developing surface wave [*Huba*, 1996b; *Otto and Fairfield*, 2000]. Again, progressive

changes in plasma properties are likely to be found further inward from the boundary because of the higher admixture of magnetospheric plasma. In the present case, the surface waves could not yet have developed into the nonlinear stage so that this mechanism is unlikely.

In the context of impulsive penetration, penetration depths of the order of $1\,R_E$ and traveling distances of a few R_E through the magnetosphere appear plausible despite filament erosion [*Lemaire and Roth*, 1991]. Impulsive penetration at the tail flanks has never been studied, so that it is not known what a flank-penetrating filament would look like. In the subsolar penetration context, the dipolar electric field that is the result of the self-polarization of the filament moving across the magnetospheric field induces a double vortex flow pattern [*Schindler*, 1979, Figure 3]. Such vortices are also seen in experiments on the propagation of neutralized ion beams [*Livesey and Pritchett*, 1989]. Simulations show similar vortices, but their cause is different, as simulations up to now have not incorporated the polarization electric field [*Echim and Lemaire*, 2000]: Vortices appear due to viscous drag, gradient B drift, and ion kinetic effects. In contrast with the subsolar case, the observations presented here reveal the presence of a vortex that always has the same sense of rotation; tail flank penetration scenarios should explain this. It is known from experiments that in some cases the magnetic field can pervade the penetrating plasma quite rapidly [*Wessel et al.*, 1988], but it is not clear what these results imply for plasma filaments at the magnetospheric boundary. This question has up to now not been addressed in impulsive penetration theory, which has mostly considered the low beta limit [*Echim and Lemaire*, 2000]. An MHD approach would attribute the changing magnetic field orientation inside the entity to Alfvén waves that propagate from the filament surface to its interior. During the 120 s traveling time of transient B, for instance, such Alfvén waves ($v_A < 500\,\mathrm{km\,s^{-1}}$ for a 20 nT field and $1\,\mathrm{cm^{-3}}$ density) could have traveled at most $9\,R_E$, implying an initial north-south extent of at most $18\,R_E$. At the same time the plasma progressively dilutes as it distends along the geomagnetic field due to the mobility of the particles along the field lines. This might be reflected by the nonzero V_z inside the transients.

Whatever the formation mechanism, the progressive braking of the filaments must be explained too. Adiabatic braking (conversion of macroscopic flow energy of the penetrating plasma into thermal energy due to the conservation of the magnetic moment in an increasing magnetic field [*Lemaire*, 1985]) could play a role if the magnetospheric field diffuses fast enough into the filament. In the crossing studied here, however, the magnetospheric magnetic field is smaller than that in the magnetosheath, so that an adiabatic acceleration and simultaneous cooling of the plasma are expected, but these are not observed. Nonadiabatic braking caused by ionospheric dissipation due to the closure of the current system driven by the $\mathbf{V} \times \mathbf{B}$ electromotive force generated by the moving filament [*Lemaire*, 1977] can operate once an electromagnetic connection to the ionosphere is established. As the magnetospheric Alfvén speed is 1000–2000 $\mathrm{km\,s^{-1}}$, the corresponding timescale is 90–180 s (less if the plasma entity originally had a larger north-south extent). The observations show a progressive deceleration from transient B on, consistent with this braking mechanism. Another nonadiabatic braking mechanism could be the local viscous interaction of the filament with its environment due to wave-particle interactions or small-scale instabilities of the filament interface.

4. Discussion

We have examined in detail the transient features observed during the February 15-16, 1996, dusk side magnetospheric boundary crossing by Magion-4 and Interball-Tail. We have attempted to interpret the observations in the framework of two different geometries. (1) In the context of a wavy magnetospheric boundary, the observations suggest a MP/LLBL with variable thickness of $\sim 1\,R_E$ with a magnetopause undulating over $0.4\,R_E$ and a stronger inner edge waviness with amplitude $0.9\,R_E$. The surface wave has a period of $\sim$450 s and a wavelength of about $10\,R_E$. Given the point of observation, the wave is still at an early stage of evolution in the sense that nonlinear effects are not believed to be present yet. We have identified the flow and magnetic field vortices in a reference frame moving with the wave phase velocity as predicted by theory. The evidence suggests that we are dealing with a Kelvin-Helmholtz instability of the equatorial dusk side inner edge (the traveling LLBL vortices model [*Sckopke et al.*, 1981]), modulated to some extent by solar wind pressure fluctuations (although no major fluctuations have been observed). (2) In the context of geometrically isolated plasma entities, the observations point to elongated entities measuring 2-4 R_E in the direction parallel to the magnetospheric boundary and 0.5-1 R_E across and with a north-south extent originally of a few R_E but possibly gradually expanding along the field lines. They penetrate up to $1\,R_E$ deep and can travel at least several R_E tailward inside the magnetosphere. As their penetration depth is not much larger than their transverse thickness, it is difficult to assert whether they are geometrically isolated from the boundary layer. The magnetic flux rope signature along the magnetospheric field and the absence of D-shaped distributions indicate that these transients are magnetically disconnected from the magnetosheath [*Vaisberg et al.*, 1998]. It is unlikely that these filaments have been produced by nonlinear development of a surface wave. An FTE-like interpretation appears consistent with the observations, although reconnection appears to have stopped; Figure 6 could then be interpreted as evidence for FTEs with a noncircular shape and a rotating core. Impulsive penetration also is a possibility; Figure 6 would then reveal the flux rope structure and the flow pattern of the penetrating filament. Nonadiabatic braking mechanisms must be invoked to explain the observed deceleration of the plasma entities. Encountering that many events during the boundary crossing studied here suggests that the circumstances for plasma entry must have been particularly favorable. Especially the periodicity of the events seems puzzling. Note also that owing to their small flux signature, events B,

C, and D are not really included in the cross correlation, so that the periodicity reflected in the cross correlation does not necessarily imply that these events are periodic. Nevertheless, one could imagine, for instance, quasi-periodic reconnection to occur if the magnetosheath field orientation would periodically reach an appropriate direction to trigger a reconnection pulse. Such periodic field changes might be produced by waves in the magnetosheath.

On the basis of geometric information alone, even the two-satellite data are not sufficient to rule out the surface wave or the isolated plasma entity hypothesis for the February 15–16, 1996, crossing. We have identified velocity vortices and magnetic flux tubes filled with magnetosheath-like plasma at or near the magnetospheric boundary, but such flux tubes are present in both scenarios. *Sibeck and Smith* [1992] already noted the ambiguity inherent in the interpretation of the flow signatures of boundary waves and FTE flux tubes. This ambiguity also has led people to reinterpret LLBL pulses originally ascribed to waves as FTEs [*Saunders*, 1983]. It is mainly the apparent periodicity of the events that strongly points to surface waves, and that is hard to explain otherwise. Our findings put the earlier isolated plasma interpretation [*Vaisberg et al.*, 1998] in a broader context. Multisatellite observations, with the spacecraft properly spaced, could shed more light on this issue. Even if we would find, for instance, that these filaments are isolated structures, we still would not know by which mechanism they were formed.

There is clearly a lack of understanding of the proposed formation mechanisms. The physics of initiation and development of FTEs and other types of patchy nonsteady reconnection is still not well known. Impulsive penetration at the flank magnetopause has not yet been studied. It is also not known how an isolated plasma entity embedded in the magnetosphere evolves: How does it expand along the field lines? How does the magnetospheric field pervade the plasma entity? How is the filament slowed down? What is the influence of the flow shear at the magnetospheric flanks on plasma entry? Simulations should eliminate formation mechanisms by demonstrating whether they can or cannot reproduce, for instance, the observation of a single flow vortex rotation sense, the characteristic timescale of magnetic field penetration into the plasma entity, the elongated shape of the filaments, the absence of adiabatic braking. Simulations might thus prove invaluable for resolving the question of the origin of the observed transients.

Acknowledgments. The authors thank S. Klimov, S. Romanov, and M. Nozdrachev for access to Interball-Tail MFI data, Y. Yermolaev for the CORALL data, and J.-A. Sauvaud for the ELECTRON data. The authors also thank M. Echim for interesting discussions. O.V., V.S., and L.A. were supported by NASA grant NAG5-4130. J.D.K., F.D. and M.R. acknowledge the support by ESA/PRODEX (Cluster II) and by the Belgian Federal Services for Scientific, Technological and Cultural Affairs.

Michel Blanc thanks David Sibeck and another referee for their assistance in evaluating this paper.

References

Berchem, J., and C. T. Russell, The thickness of the magnetopause current layer: ISEE 1 and 2 observations, *J. Geophys. Res., 87,* 2108–2114, 1982.

Berchem, J., and C. T. Russell, Flux transfer events on the magnetopause: Spatial distribution and controlling factors, *J. Geophys. Res., 89,* 6689–6703, 1984.

Echim, M. M., and J. F. Lemaire, Laboratory and numerical simulations of the impulsive penetration mechanism, *Space Sci. Rev., 92,* 565–601, 2000.

Fairfield, D. H., A. Otto, T. Mukai, S. Kokubun, R. P. Lepping, J. T. Steinberg, A. J. Lazarus, and T. Yamamoto, Geotail observations of the Kelvin-Helmholtz instability at the equatorial magnetotail boundary for parallel northward fields, *J. Geophys. Res., 105,* 21,159–21,173, 2000.

Farrugia, C. J., et al., Coordinated Wind, Interball/Tail, and ground observations of Kelvin-Helmholtz waves at the near-tail, equatorial magnetopause at dusk: January 11, 1997, *J. Geophys. Res., 105,* 7639–7667, 2000.

Fitzenreiter, R. J., and K. W. Ogilvie, Kelvin-Helmholtz instability at the magnetopause: Observations, in *Physics of the Magnetopause, Geophys. Monogr. Ser.*, vol. 90, edited by P. Song, B. U. O. Sonnerup, and M. F. Thomsen, pp. 277–283, AGU, Washington, D. C., 1995.

Huba, J.D., Impulsive plasmoid penetration of a tangential discontinuity: Two-dimensional ideal and Hall magnetohydrodynamics, *J. Geophys. Res., 101,* 24,855–24,868, 1996a.

Huba, J.D., The Kelvin-Helmholtz instability: Finite Larmor radius magnetohydrodynamics, *Geophys. Res. Lett., 23,* 2907–2910, 1996b.

Hubert, D., C. C. Harvey, M. Roth, and J. De Keyser, Electron density at the subsolar magnetopause for high magnetic shear: ISEE 1 and 2 observations, *J. Geophys. Res., 103,* 6685–6692, 1998.

Ivchenko, N. V., D. G. Sibeck, K. Takahashi, and S. Kokubun, A statistical study of the magnetosphere boundary crossings by the Geotail satellite, *Geophys. Res. Lett., 27,* 2881–2884, 2000.

Kivelson, M. G., and S.-H. Chen, The magnetopause: Surface waves and instabilities and their possible dynamical consequences, in *Physics of the Magnetopause, Geophys. Monogr. Ser.*, vol. 90, edited by P. Song, B. U. O. Sonnerup, and M. F. Thomsen, pp. 257–268, AGU, Washington, D. C., 1995.

Klimov, S., et al., ASPI experiment: Measurements of field and waves onboard Interball Tail mission, in *Interball Mission and Payload, rep. CNES-IKI-RSA*, pp. 120–152, CNES, Paris, 1995.

Ku, H. C.. and D. Sibeck, Flux transfer events produced by the onset of merging at multiple X lines, *J. Geophys. Res., 105,* 2657–2675, 2000.

Lemaire, J., Impulsive penetration of filamentary plasma elements into the magnetospheres of the Earth and Jupiter, *Planet. Space Sci., 25,* 887–890, 1977.

Lemaire, J., Plasmoid motion across a tangential discontinuity (with application to the magnetopause), *J. Plasma Phys., 33,* 425–436, 1985.

Lemaire, J., and M. Roth, Penetration of solar wind plasma elements into the magnetosphere, *J. Atmos. Terr. Phys., 40,* 331–335, 1978.

Lemaire, J., and M. Roth, Non-steady-state solar wind–magnetosphere interaction, *Space Sci. Rev., 57,* 59–108, 1991.

Livesey, W. A., and P. L. Pritchett, Two dimensional simulations of a charge-neutral plasma beam injected into a transverse magnetic field, *Phys. Fluids B, 1,* 914, 1989.

Ma, Z. W., J. G. Hawkins, and L. C. Lee, A simulation study of impulsive penetration of solar wind irregularities into the magnetosphere at the dayside magnetopause, *J. Geophys. Res., 96,* 15,751–15,765, 1991.

Miura, A., Dependence of the magnetopause Kelvin-Helmholtz instability on the orientation of the magnetosheath magnetic field, *Geophys. Res. Lett., 22,* 2993–2996, 1995.

Miura, A., and P. L. Pritchett, Nonlocal stability analysis of the MHD Kelvin-Helmholtz instability in a compressible plasma, *J. Geophys. Res., 87,* 7431–7444, 1982.

Ogilvie, K. W., and R. J. Fitzenreiter, The Kelvin-Helmholtz instability at the magnetopause and inner boundary layer surface, *J. Geophys. Res., 94,* 15,113–15,123, 1989.

Otto, A., and D. H. Fairfield, The Kelvin-Helmholtz instability at the magnetotail boundary: MHD simulation and comparison with Geotail observations, *J. Geophys. Res., 105,* 21,175–21,190, 2000.

Phan, T. D., and G. Paschmann, Low-latitude magnetopause and boundary layer for high magnetic shear, 1, Structure and motion, *J. Geophys. Res., 101,* 7801–7815, 1996.

Russell, C. T., and R. C. Elphic, Initial ISEE magnetometer results: Magnetopause observations, *Space Sci. Rev., 22,* 681–715, 1978.

Russell, C. T., and R. C. Elphic, ISEE observations of flux transfer events at the dayside magnetopause, *Geophys. Res. Lett., 6,* 33–36, 1979.

Safrankova, J., G. Zastenker, Z. Nemecek, A. Fedorov, M. Simersky, and L. Prech, Small-scale observation of magnetopause motion: preliminary results of the INTERBALL project, *Ann. Geophys., 15,* 562–569, 1997.

Saunders, M. A., Recent ISEE observations of the magnetopause and low latitude boundary layer: A review, *J. Geophys., 52,* 190–198, 1983.

Sauvaud, J.-A., et al., The ELECTRON experiment: A top hat spectrometer for the Tail Probe, in *Interball Mission and Payload, rep. CNES-IKI-RSA,* pp. 153–169, CNES, Paris, 1995.

Sauvaud, J.-A., P. Koperski, T. Beutier, H. Barthe, C. Aoustin, J. J. Thocaven, J. Rouzaud, E. Penou, O. L. Vaisberg, and N. Borodkova, The INTERBALL-Tail ELECTRON experiment: Initial results on the low-latitude boundary layer of the dawn magnetosphere, *Ann. Geophys., 15,* 587–595, 1997.

Savoini, P., M. Scholer, and M. Fujimoto, Two-dimensional hyprid simulations of impulsive plasma penetration through a tangential discontinuity, *J. Geophys. Res., 99,* 19,377–19,391, 1994.

Schindler, K., On the role of irregularities in plasma entry into the magnetosphere, *J. Geophys. Res., 84,* 7257–7266, 1979.

Sckopke, N., G. Paschmannn, G. Haerendel, B. U. Ö. Sonnerup, S. J. Bame, T. G. Forbes, E. W. Hones Jr., and C. T. Russell, Structure of the low-latitude boundary layer, *J. Geophys. Res., 86,* 2099–2110, 1981.

Seon, J., L. A. Frank, A. J. Lazarus, and R. P. Lepping, Surface waves on the tailward flanks of the Earth's magnetopause, *J. Geophys. Res., 100,* 11,907–11,922, 1995.

Sibeck, D. G., A model for the transient magnetospheric response to sudden solar wind dynamic pressure variations, *J. Geophys. Res., 95,* 3755–3771, 1990.

Sibeck, D. G., and M. F. Smith, Magnetospheric plasma flows associated with boundary waves and flux transfer events, *Geophys. Res. Lett., 19,* 1903–1906, 1992.

Sibeck, D. G., et al., Plasma transfer processes at the magnetopause, *Space Sci. Rev., 88,* 207–283, 1999.

Sibeck, D. G., L. Prech, J. Safrankova, and Z. Nemecek, Two-point measurements of the magnetopause: Interball observations, *J. Geophys. Res., 105,* 237–244, 2000.

Song, P., and C. T. Russell, Time series data analyses in space physics, *Space Sci. Rev., 87,* 387–463, 1999.

Song, P., R. C. Elphic, and C. T. Russell, ISEE 1 and 2 observations of the oscillating magnetopause, *Geophys. Res. Lett., 15,* 744–747, 1988.

Sonnerup, B. U. Ö., and M. Scheible, Minimum and maximum variance analysis, in *Analysis Methods for Multi-Spacecraft Data, ISSI SR-001,* edited by G. Paschmann and P. W. Daly, pp. 185–220, International Space Science Institute, Bern, 1998.

Vaisberg, O. L., et al., Complex plasma analyzer SCA-1, in *Interball Mission and Payload, rep. CNES-IKI-RSA,* pp. 170-177, CNES, Paris, 1995.

Vaisberg, O. L., V. N. Smirnov, L. A. Avanov, J. H. Waite Jr., J. L. Burch, C. T. Russell, A. A. Skalsky, and D. L. Dempsey, Observation of isolated structures of the low latitude boundry layer with the INTERBALL/Tail probe, *Geophys. Res. Lett., 25,* 4305–4308, 1998.

Walker, A. D. M., The Kelvin-Helmholtz instability in the low latitude boundary layer, *Planet. Space Sci., 29,* 1119–1133, 1981.

Wessel, F. J., R. Hong, J. Song, A. Fischer, N. Rostoker, A. Ron, R. Li, and R. Y. Fan, Plasmoid propagation in a transverse magnetic field and in a magnetized plasma, *Phys. Fluids, 31,* 3778–3784, 1988.

Yermolaev, Y. I., A. O. Fedorov, O. L. Vaisberg, V. M. Balebanov, Y. A. Obod, R. Jimenez, J. Fleites, L. Llera, and A. N. Omelchenko, Ion distribution dynamics near the Earth's bow shock: First measurements with the 2D ion spectrometer CORALL on the INTERBALL/Tail-probe satellite, *Ann. Geophys., 15,* 533–541, 1997.

M. Roth, F. Darrouzet, and J. De Keyser, Belgian Institute for Space Aeronomy, Ringlaan 3, B-1180 Brussels, Belgium. (Michel.Roth@oma.be, Fabien.Darrouzet@oma.be, Johan.DeKeyser@oma.be)

L. Avanov, N. Rybjeva, V. Smirnov, and O. L. Vaisberg, Space Research Institute, 84/32 Profsoyuznaya, 117810 Moscow, Russia. (lavanov@iki.rssi.ru, nata@iki.rssi.ru, vsmirnov@iki.rssi.ru, olegv@iki.rssi.ru)

Z. Nemecek and J. Safrankova, Space Physics Group, Faculty of Mathematics and Physics, Charles University, V Holeoviekach 2, Praha 8, 180 00, Czech Republic. (NEMECEK@aurora.troja.mff.cuni.cz, SAFR@aurora.troja.mff.cuni.cz)

(Received June 6, 2000; revised March 9, 2001;
accepted March 9, 2001.)